Wind- Driven Airflow through Building Openings: Preliminary Experimental Results Using Particle Image Velocimetry

Lo, Liang Chung (James)

Engineering Laboratory, National Institute of Standards and Technology
100 Bureau Drive Gaithersburg, MD 20899

Submitted to and presented at:
ASHRAE Annual Conference
Seattle WA, July 2, 2014

U.S. Department of Commerce
Penny Pritzker, Secretary of Commerce

National Institute of Standards and Technology
Willie E May, Acting Director

DISCLAIMERS

Certain commercial entities, equipment, or materials may be identified in this document in order to describe an experimental procedure or concept adequately. Such identification is not intended to imply recommendation or endorsement by the National Institute of Standards and Technology, nor is it intended to imply that the entities, materials, or equipment are necessarily the best available for the purpose.

Any link(s) to website(s) in this document have been provided because they may have information of interest to our readers. NIST does not necessarily endorse the views expressed or the facts presented on these sites. Further, NIST does not endorse any commercial products that may be advertised or available on these sites.

Wind-driven Airflow through Building Openings: Preliminary Experimental Results using Particle Image Velocimetry

L. James Lo, PhD
Member ASHRAE

ABSTRACT

Today's low energy and sustainable buildings often call for innovative designs involving strategies such as natural ventilation. However, natural ventilation airflow is often difficult to estimate, mostly due to the unsteadiness of the wind. This study investigates wind-driven natural ventilation experimentally by using particle image velocimetry (PIV) conducted in a boundary layer wind tunnel using a glass building analogue with modeled openings. Using the PIV technique, both the outdoor wind flow and the resulting indoor through flow were visualized and measured. By varying the opening sizes in the glass model and the incident angle of the approaching wind, the airflow behavior around the openings was investigated. The experimental results provide a novel representation of the airflow characteristics for wind-driven airflow through a building, and the results are expected to aid designers in estimating wind-driven ventilation rates in buildings.

INTRODUCTION

With today's focus on low energy and sustainable buildings, building designers, engineers and researchers are increasingly proposing to incorporate natural ventilation in innovative building designs. Despite these interests and the progress to date, one key component of natural ventilation, i.e., the wind, has proven to be a difficult problem due to its unsteady nature. One difficulty with predicting wind-driven airflow is the determination of the fundamental fluid mechanics involved around the ventilation openings. While it is common practice to model the airflow though building openings as simple pressure-driven pipe flows with specific discharge coefficients for individual openings (orifice equation, (Karava et al., 2007)), this practice cannot be utilized when the openings become large. Even with this knowledge, it is not clear when the transition between small opening flow (pressure-driven pipe flow) and large opening flow (momentum driven flow preserving wind characteristics) occurs. Researchers have assumed small openings to be roughly 2 % of wall porosity (Chang and Meroney, 2001), with large openings over 15 % wall porosity (Seifert et al., 2006). These assumptions leave a large grey area for many typical building openings (e.g. windows and doors).

To investigate this issue, experiments were conducted using a boundary layer wind tunnel, particle image velocimetry (PIV) and a glass building model with openings to simulate wind-driven flow through a building. Using the PIV technique, both the simulated outdoor wind flow and the resulting indoor cross ventilation flow can be visualized and measured through the glass model. By varying the opening sizes in the glass model and the incident angle of the approaching wind, the fluid behavior around the openings was investigated. While the complete experimental results will provide a novel

James Lo is a NRC Postdoctoral Research Associate in the Indoor Air Quality and Ventilation Group, Energy and Environment Division, National Institute of Standards and Technology (NIST), Gaithersburg, Maryland.

representation of the airflow characteristics for wind-driven flow through a building, the study is still ongoing and only partial preliminary results are presented in this paper.

METHODOLOGY

While PIV investigation of wind-driven airflow had been conducted by Karava et al. (2011), the previous study only focuses on various opening locations in the vertical plane along the center of the windward and leeward walls. This current investigation focuses not on the opening location, but on the effect of building opening size and wind incident angle on wind-driven ventilation using the PIV technique, a novel approach to study such problems. This study also marks the first attempt to use glass-built models to improve data quality for the PIV image. The glass model was placed inside a recirculating boundary layer wind tunnel to simulate specific airflows required for the experiment. The schematic diagram for the experimental setup **is shown in Figure 1**

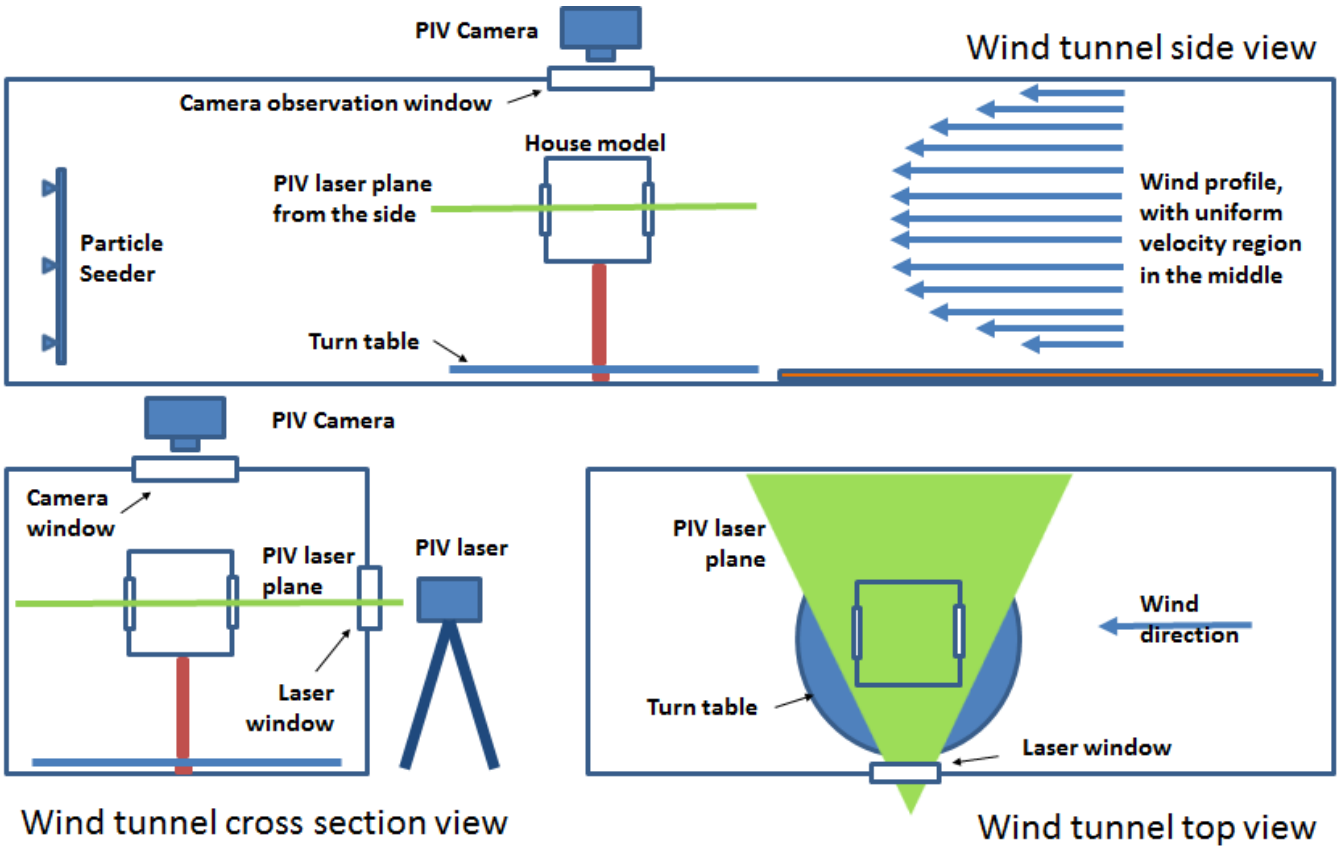

Figure 1 Experimental setup (not to scale). The glass model is place on a raised platform to reach the uniform velocity region of the wind tunnel, while the PIV laser projects the laser sheet parallel to the ground from the side, and the PIV camera observes the area of interest from the top of the wind tunnel through an observation window.

The glass models

Four glass cubes with 10 cm (3.94 in.) sides were constructed for the experiment, modelling a 2 meter (6.56 ft) real size cube building at 1/20 scale. Each glass cube has two identical square openings, placed in center of the opposite walls; with the sizes varying between the models at 2 %, 5 %, 10 % and 15 % wall porosity. Wall porosity is defined as the ratio

between the area of the opening and the wall surface for the given façade. The corresponding opening sizes used are tabulated in **Table 1.** Un-tinted quartz glass is used for its optical quality relative to window glass or poly-methyl methacrylate (acrylic glass). A photograph of one of the glass cubes **is shown in Figure 2**.

Table 1. Model openings

Wall Porosity	Opening side length (SI, cm)	Opening side length (I-P, inch)
2 %	1.4	0.55
5 %	2.2	0.87
10 %	3.2	1.26
15 %	3.9	1.54

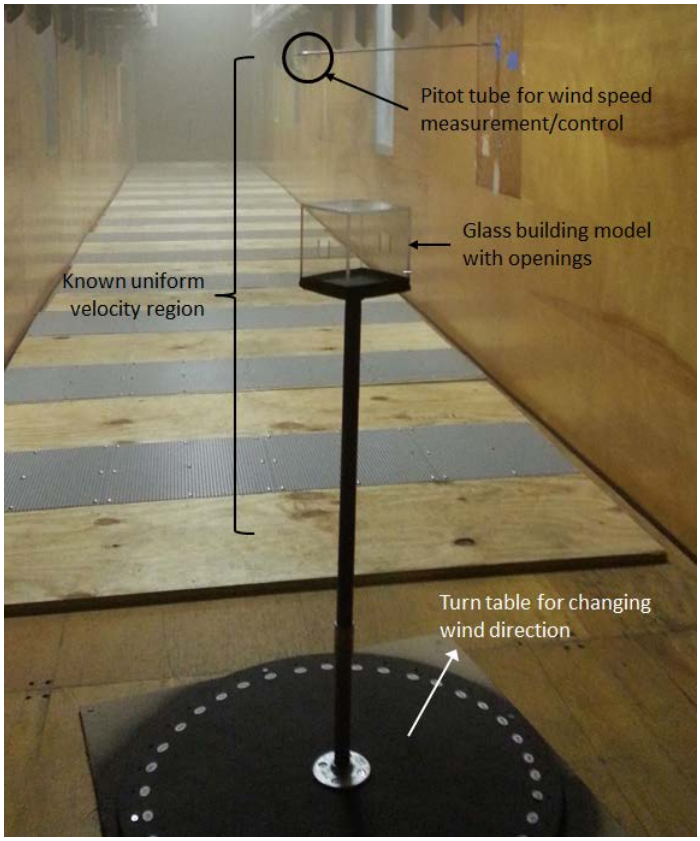

Figure 2 Experimental setup inside the wind tunnel, including the turntable, the elevated stand, the glass model, and pitot tube used for measuring the wind tunnel speed

Wind Tunnel Setup

For the current stage of investigation, a uniform wind velocity profile with little turbulence is required for studying the sole effect of opening sizes and wind incident angle. This uniform velocity profile is significantly different than the typical atmosphere boundary layer (ABL) profile, which theoretically takes a power law based shape. While the resulting flow field and flow rate might not be directly comparable to the other studies using ABL, the wind directions and opening sizes is better examined due to the lack of interference from ABL. This specific wind condition was achieved in the NIST Physical

Measurement Laboratory's Fluid Metrology wind tunnel (T. T. Yeh and J. M. Hall, n.d.), which provides a uniform velocity profile in the middle of the test section (averaging ± 0.1 m/s, 3.9 in./s), low turbulence intensity (2 %) and airspeed control precision of ± 0.01 m/s (± 0.4 in./s) using a pressure/temperature/relative humidity feedback control loop. With the capability for providing a stable wind velocity profile at various speeds, the velocities shown in Table 2 were chosen.

Table 2. Wind Tunnel Velocities

Wind Case	Velocity (SI, m/s)	Velocity (I-P, ft/s)
1	1.00	3.28
2	2.00	6.56
3	3.00	9.84
4	4.00	13.1
5	5.00	16.4

The upper velocity constraint of 5 m/s (16.4 ft/s) was imposed due to the small vibration caused by the wind tunnel operation. The vibration introduces additional movement in the PIV image and renders the image unusable at higher speeds. One difficulty introduced by the inability to increase the wind velocity is the failure to achieve dynamic similarity using the 1/20 scaled model as the wind tunnel speed is similar to the full scale wind. However, Cermak (1995) stated that wind tunnel testing for buildings have always suffered such problem as the building model scales are usually extremely small while upper wind tunnel speed is limited. The concept of Reynolds Number Independence is used for wind tunnel testing for buildings, which ignores the similarity for high frequency turbulence, as long as the mid frequency turbulence which concerns buildings were matched.

The wind tunnel setup also involved the installation of the temporary turn-table (**See Figure 2**) for varying the wind incident angle. Due to the symmetry of the model (see the glass model section), only one-quarter of the possible wind incident angles (wind direction) were tested, from 0 degree to 90 degree in 10 degree intervals. Between the three parameters tested (opening size, wind direction and wind velocity), a total of 200 test cases are planned. At this time, 70 selected tests have been completed.

Figure 2 also shows one of the glass models being tested, with the model elevated from the turn-table using a round steel pipe for support. The steel pipe eliminated most of the subtle vibration from the wind pressure, which otherwise could further affect the PIV image quality.

PIV Setup

The particle image velocimetry system used in this project consists of one pair of Class 4 (200 mJ per pulse) Nd:YAG lasers at 532 nm wavelength with a sheet forming optical lens, a high speed camera with a band pass filter for the 532 nm wavelength, particle seeders, and software to facilitate all the hardware. The setup schematic was described previously in **Figure 1**, where the lasers were installed on the side of the wind tunnel with the laser light sheet parallel to the ground and the camera was installed above the glass to obtain the image for the flow field. **Figure 3** shows photographs of the installation. The seeding criteria follows Melling's (1997) suggestion and 1 um particle size were used for PIV, and 10 μm particles were used for visualization images. Each PIV investigation include 30 pairs of high speed images with 250 us time step. The resulting velocity profile is the average of 30 image pairs. The specific interrogation and post processing methods are currently being tested and developed, and only preliminary results and visualization images are included in this paper.

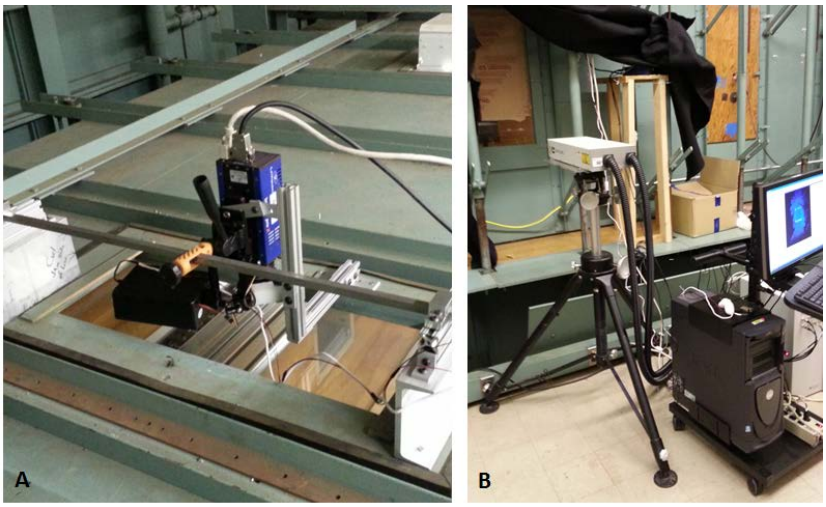

Figure 3 (a) PIV camera installed on the top of the wind tunnel with the observation window, and (b) the PIV laser located on the side of the wind tunnel shooting laser light sheet into the wind tunnel

RESULTS

Verification of the PIV Image Data

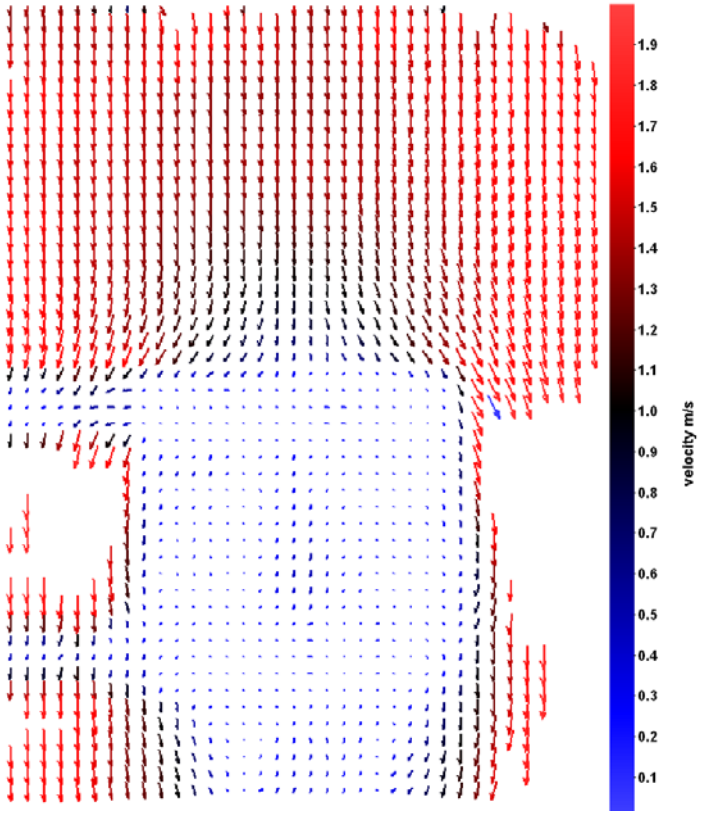

Figure 4 PIV results of airflow velocity vectors on the xy plane for the test case 2 % wall porosity, 2 m/s wind speed and 0 degree wind direction. The glass model area is readily visible as the white/blue square in the middle.

The first requirement for the study was to provide a stable uniform wind velocity profile approaching the glass model in order to study the flow characteristics strictly affected by the experimental parameters (wind velocity, wind direction and opening sizes). It is important then to examine the PIV results to determine whether such uniformity has been achieved. Unfortunately, due to the limited camera view field, the furthest upwind area of the image is within one characteristic length of the glass model, therefore the upwind flow field is affected by the model and does not represent the free stream velocity field. While the velocity profile cannot be verified directly, an example PIV result, obtained at 2 m/s (6.56 ft/s) with 0 degree wind direction and 2 % wall porosity (**Figure 4**), shows the average velocity of the airflow approaching the model is stable and uniform, suggesting the required test condition has been met. The qualitative agreement also suggests the PIV method used produces credible results.

Evidence of pressure driven flow

While insufficient data have been analyzed to identify the transition point between the pressure driven and momentum driven airflow at this time, qualitative verification of previous assumptions has been accomplished. For example, the 2 % opening case at 10 degree wind direction and 2 m/s wind speed (**Figure 5b**) yields a visible jet that is perpendicular to the wall surface in the smoke visualization image, a phenomenon that only happens if a complete pressure driven flow is present. As the wind incident angle increases, however, the jet destabilized and tilted, resulting in an airflow that is not purely driven by the static pressure around the opening. Such results are most likely produced by significant pressure difference around the opening as the wind incident angle increases. Additional experiments are planned to study the flow shape inducing mechanism and the possible impact on indoor flow field estimation.

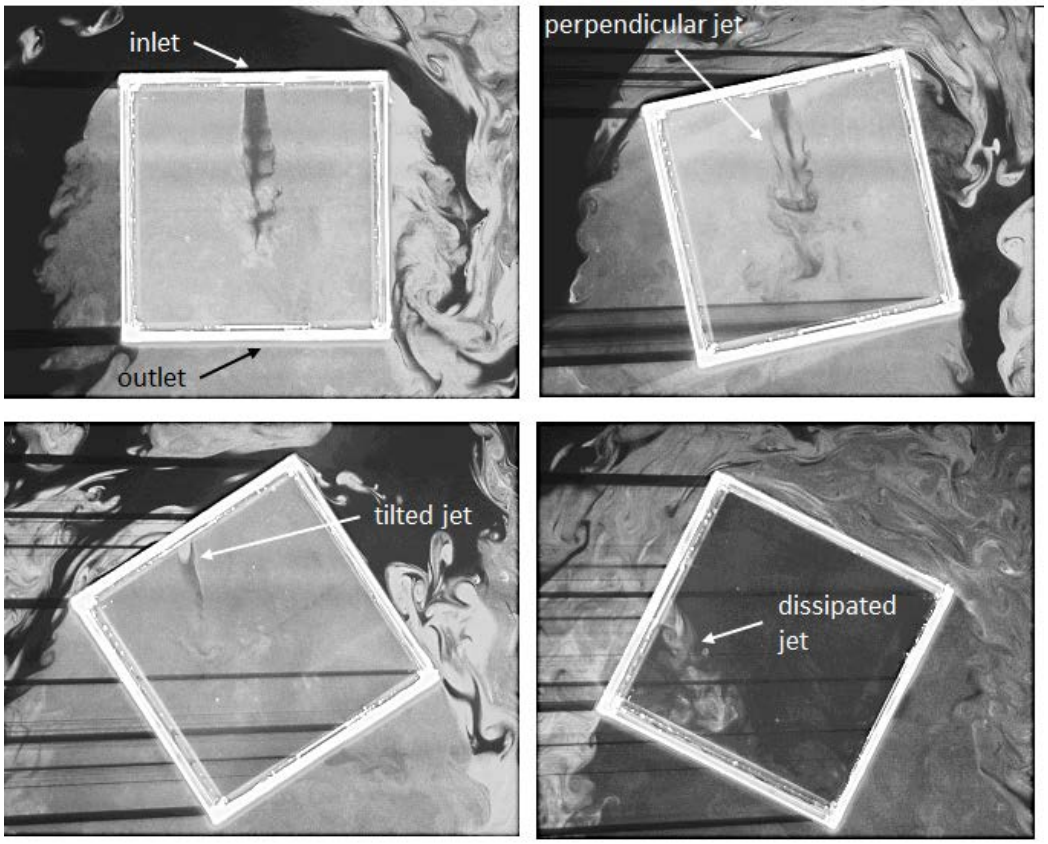

Figure 5 Flow visualization of the 2 % wall porosity test cases at 2 m/s wind speed (wind tunnel airflow from top to bottom) with variation in wind direction (a) 0 degree (b) 10 degree (c) 30 degree (d) 60 degree

Evidence of momentum driven flow

As the opening becomes larger, the visualization images in **Figure 6** show that the momentum based flow starts to dominate. In **Figure 6a**, where the opening size is at 2 % wall porosity, the small opening pressure driven jet is still evident. When the opening size increases to 5 % in **Figure 6b,** the additional eddies entering from outside of the cube become visible. When the opening size increases to 15 % in **Figure 6d**, there seems to be no sign of pressure driven jet left.

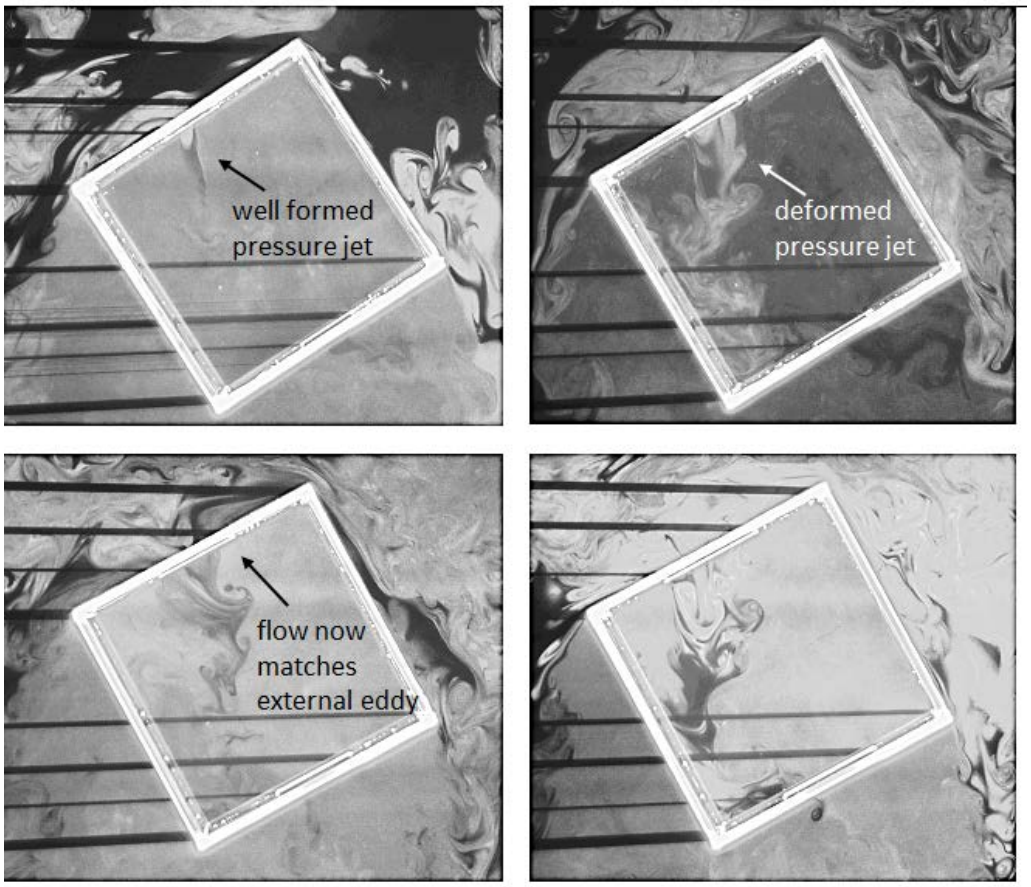

Figure 6 Flow visualization of the 30 degree test cases at 2 m/s wind speed (wind tunnel airflow from top to bottom) with variation in opening sizes (a) 2 % (b) 5 % (c) 10 % (d) 15 %

DISCUSSIONS

Transition between momentum and pressure driven flow

From visual inspection, the evidence provided in **Figure 6** is consistent throughout all the test cases, places the transition point between the pressure and momentum driven flows somewhere between 2 % and 5 % wall porosity. While further PIV analysis will provide more quantitative data to formulate a model of such transition, it is difficult to experimentally obtain the exact transition wall porosity due to accuracy required to survey small changes in opening size between 2 % and 5 %. A computational fluid dynamics (CFD) investigation could provide the necessary accuracy for virtual experimentation, while using the PIV data for validation purposes.

Implications on natural ventilation flow estimation

As mentioned in the Introduction, the typical estimation of wind driven natural ventilation flow assumes a simple

pressure driven pipe flow and employees the orifice equation, as seen in ASHRAE Handbook Fundamentals (2009), chapter 16. Without precise pressure data on building façades, an engineer might also consult chapter 24, airflow around the building, to estimate the pressure at the façade as the driving force for the ventilation flow. However, this process's base assumption is that the airflow is pressure driven. As the visualization in **Figure 5 and 6** imply, this assumption would only be valid at very low wall porosity. Since most intentional openings, such as windows, are potentially larger than 2 % wall porosity, estimating wind-driven flow rate using the pressure assumption could be subject to significant error.

Experimental challenges

One of the key issues with the PIV technique is the problem with determining the measurement uncertainty. As Cao et al. (2014) noted in the PIV review paper for indoor airflow measurement, the technique is prone to position induced errors due to complication in experimental setup. Besides the possible errors mentioned by Cao et al., additional obstacles were discovered in this experiment, specifically associated with the optical quality of the PIV setup.

In **Figure 4** there are clearly missing PIV data (the empty regions) in both the left and right areas of the model. This is due to the reflection of the model surface, which created a brighter area near the laser inlet (right side of the figure), and a darker spot near the outlet (left side of the figure). The specific bright/dark areas due to reflection could be reduced by using a wavelength-specific filter coating on the glass. Additionally, as seen in Figure 6, there are several dark streaks on the left side of each image. These streaks are laser shadows cast from the edges of glass in the model, which also affect the data PIV data quality in those areas. Additional polishing on all glass edges could possibly reduce such shadowing, as well as repositioning of the laser parallel to most edges. These improvements will be considered in the future work.

CONCLUSION

PIV investigation of wind-driven natural ventilation airflow was conducted in a wind tunnel using a glass model. The preliminary results indicate the PIV technique can be used to investigate the effect of wind direction and opening sizes on the ventilation flow. Qualitative visualization suggested the transition opening size from pressure to momentum based airflow is over 2 % but smaller than 5 % wall porosity, although only applicable to conditions tested. Such small opening size implies that pressure based airflow assumption might not be correct when estimating wind-driven natural ventilation airflow through a building. Further analysis and expanded CFD based parametric analysis will provide data for ongoing modelling effort to more accurately describe the interactions between the factors impact such transition over wider range.

REFERENCES

ASHRAE, 2009. ASHRAE Handbook. Fundamentals. American Society of Heating, Refrigerating and Air-Conditioning Engineers, Atlanta.

Cao, X., Liu, J., Jiang, N., Chen, Q., 2014. Particle image velocimetry measurement of indoor airflow field: A review of the technologies and applications. Energy Build. 69, 367–380.

Cermak, J.E., Cochran, L.S., Leflier, R.D., 1995. Wind-tunnel modelling of the atmospheric surface layer. J. Wind Eng. Ind. Aerodyn. 54–55, 505–513.

Chang, C.-H., Meroney, R.N., 2001. Numerical and physical modeling of bluff body flow and dispersion in urban street canyons. J. Wind Eng. Ind. Aerodyn. 89, 1325–1334.

Karava, P., Stathopoulos, T., Athienitis, A.K., 2007. Wind-induced natural ventilation analysis. Sol. Energy 81, 20–30.

Karava, P., Stathopoulos, T., Athienitis, A.K., 2011. Airflow assessment in cross-ventilated buildings with operable façade elements. Build. Environ. 46, 266–279.

Melling, A., 1997. Tracer particles and seeding for particle image velocimetry. Meas. Sci. Technol. 8, 1406.

Seifert, J., Li, Y., Axley, J., Rösler, M., 2006. Calculation of wind-driven cross ventilation in buildings with large openings. J. Wind Eng. Ind. Aerodyn. 94, 925–947.

T. T. Yeh, J. M. Hall, n.d. Air Speed Calibration Service (Special Publication No. 250-79), Special Publication. National Institute of Standards and Technology.